MVA2007 IAPR Conference on Machine Vision Applications, May 16-18, 2007, Tokyo, JAPAN

An unsupervised learning approach based on Hopfield-like network for assessing posterior capsule opacification

Naoufel Werghi
College of Information Technology
University of Dubai
nwerghi@ud.ac.ae

Rachid Sammouda, Fatma AlKirbi
Department of Computer Sciences
University of Sharjah
{rsammouda,kfatma}@sharjah.ac.ae

Abstract

Posterior Capsule Opacification (PCO) is the commonest complication of cataract surgery occurring in up to 50% of patients by 2 to 3 years after the operation [1]. This paper proposes a new approach for the assessment of PCO digital images. The approach deploys an unsupervised learning technique for clustering image pixels into different regions based on chromatic attributes. The innovation aspect of this paper, is proposing the number of regions in a clustered image as measurement tool for assessing the PCO. The approach exhibits robustness and stability that would contribute in providing a systematic and objective assessment.

1 Introduction

Posterior Capsule Opacification (PCO) is a frequent postoperative complication that attacks the eye after undergoing a cataract extraction surgery in which the infected lens is removed and replaced by an artificial one (the intraocular lens or IOL). Such intervention is often followed by a complication, known as the Posterior Capsule Opacification, which manifests by the development of lens epithelium cells (LEC) that grow at the posterior half of the eye capsule behind the IOL. There are different types of PCO, namely fibrosis, pearls and wrinkles. Theses names reflect the type of texture produced by the LEC distribution (Figure 1). Accessing the effectiveness of the clinical trials

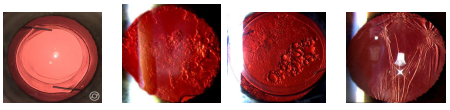

Figure 1: safe eye's capsule, eyes affected respectively with fibrosis , pearls and wrinkles PCO.

performed to reduce or inhibit PCO requires a quantitative analysis of the PCO, capable of measuring the amount of PCO in the eye's capsule with a reasonable reliability. Human assessment is often corrupted by bias, subjectivity and lack of accuracy. This happens, for instance, when comparing PCO progression by studying images taken before and after treatment and also when comparing the severity of the PCO. This issue, fuelled the investigation of image processing technique that might overcome the limitations of manual assessment, particularly with regard to subjectivity. This paper presents some steps towards an objective and reliable assessment of PCO images. It proposes a methodology for defining measurement tool that would contribute in reaching this objective.

2 Previous work

In the medical community Lasa et al [2] pioneered the exploitation of digital images for assessing PCO. The image capture system covers small portion of the capsule, requiring thus the combination of many images for a full assessment. Their analysis could only detect hazy capsules. Hayashi et al [3] assessed the PCO by means of "density" measure. Their technique uses cross-sectional images of the IOL and the posterior capsule, and thus no morphological data of the PCO is provided. Also, the ability of detecting progression of PCO and the reproducibility of the results were not documented in that work. Tetz et al [4] proposed an interactive system whereby the operator can trace manually the boundaries of the textured areas in the images. The operator subjectively assigns a severity score between 0 and 4 to each textured zone in the image. A PCO grade is then updated by summing the scores weighted by the fractional area of each zone. This method infers systematic and parallax error due to the manual processing. Ursell et al [5] proposed an automated system for detecting and measuring the presence of the PCO. The purpose of this work was to establish a relationship between intraocular lens material and the development of PCO. However no details was given on the image analysis techniques. The reliability and the validity of this system was not documented. Wang et al [6] used thresholding technique whereby a pixel is classified as belonging to the PCO area if its gray level is above a given threshold. The PCO is then assessed by the percentage of classified pixels. This method is very sensitive to the variations in illuminations and light reflections. Its main limitation however lies in the fact that by principle this technique is not qualified to segment reliably textured areas. Friedman et al [7] tried to improve this method by preprocessing the image in a first stage to reduce the effects of illumination artifacts. This enhanced to some extent the performance of the method. Yet its limitation with respect to textured

areas persisted. Baraman et al [8] applied some adhoc filtering techniques to enhance the texture of the image and then classify a pixel as being part of the PCO area based on the variance of the pixels' values in predefined neighborhood. Paplinski et al [9] proposed a segmentation approach based on the analysis of the co-occurrence matrix derived from the PCO image. The goal was to extract the textured area. The threshold setting that intervenes in the segmentation seems, however, to require some manual intervention. Siegel et al [10] proposed a similar approach, yet with some preprocessing stage that removes the flashlight reflection, based on image registration technique. In addition, the entropy of the co-occurrence matrix is proposed as direct measure of the PCO in the image. In a recent comparison [11] this method demonstrated more consistent PCO assessment than the methods of [8, 4]. Yet there was no evidence that the proposed method can handle complex and various types of PCO textures. More recently Aslam [12] confirmed the validity of the entropy measure, as mean to differentiate between different levels of PCO, provided a strict constraints on the illumination conditions.

3 The approach

It is noticed from the previous survey that most of the approaches targeted as a solution the detection of the PCO areas in the image, and eventually consider the relative size of these areas with respect to the whole image as a "measure" of the PCO amount. While theoretically this approach looks valid and justified, it raises serious problems practically. In effect, the PCO texture characterized by a high level of irregularity in terms of both scale and frequency. Attempting the extraction of such areas via a segmentation approach would be a quite difficult task, bearing in mind that the segmentation of regular texture is already a hard problem. The idea on which we build our approach, emanates from the concept of a region within a digital image. We define a region as a group of connected pixels sharing close chromatic value. In a smooth and clean image, corresponding to a safe case, the number of regions is small. Ideally such image will show a single and compact region. In the opposite, an image corresponding to PCO case, would be characterized by a relatively larger number of regions, induced by the discontinuities and variations inferred by the PCO texture. Moreover the number of regions is expected to be function of the amount of PCO, and thus can reflect its level. Assuming this hypothesis ,we propose to investigate the suitability of the number of regions as a measuring tool for assessing PCO from digital images.

the proposed paradigm consists in extracting and counting the regions in the image. The process involves a preprocessing stage whereby a circular central region is selected, covering about 40% of the whole image. According to ophthalmologists, this area is affecting the most the vision acuity. The rest of the image is considered as background. Pixels in that region are set to the average value of the area of interest. Afterwards, an unsupervised clustering technique is applied to the image. In this stage the image pixels are assigned to different classes according to their chromatic values. Next, the image is filtered to remove artifacts and tiny-regions caused by over-clustering. In the next stage, pixels in each class are grouped into sets of connected regions. Then the number of regions in each class is counted and summed-up.

The clustering aims to partition image pixels into K groups (clusters) sharing the same chromatic characteristics. The objective here is not to determine the optimal number of clusters, but rather to examine the variation of the number of regions with respect to the number of classes. We used the standard *K-means* clustering technique [13]. This technique basically searches for the optimal partition of a set of objects (e.g. pixels) ,whereby each object is represented by a vector of feature (e.g. RGB components), into a K disjoint subsets (clusters) S_l, $l = 1..K$. The optimal partition is obtained by minimizing a given objective function, usually defined by the sum of the squared distances between the object feature vectors of each subset and their centroids $\mu_l, l = 1..K$. $E = \sum_{l=1}^{K} \sum_{X_i \in S_l} \|X_i - \mu_l\|^2$

The implementation of the algorithm deployed a Hopfield-like artificial neural network, inspired from the architecture proposed in [14]. The structure of the network is composed of a $N \times K$ cells. U_{il} and V_{il} represent respectively the input and the output of the neuron associated to i^{th} pixel and l^{th} class. The network has feed-back loops from the output to the inputs. After applying a new input, the network output is calculated and fed back to the input, then the output is calculated again. The process is repeated until the output becomes constant. The network is designed to classify the image of N pixels among K classes, such that the assignment of the pixels minimizes the following objective function $E = \frac{1}{2} \sum_{i=1}^{N} \sum_{l=1}^{K} R_{il}^2 V_{il}^2$ where R_{il} is the Mahalanobis distance measure between the k_{th} pixel and the centroid of class l. The minimization is achieved by solving the motion equation: $\frac{\partial U_{il}}{\partial t} = -\alpha(t) \frac{\partial E}{\partial V_{il}}$, where $\alpha(t)$ is a scalar positive function of time used to increase the convergence of the network. It is set to $\alpha(t) = t * (T_s - t)$, where T_s is a pre-specified number of iteration.

The network classifies the feature space based on the compactness of each cluster calculated using the Mahalabonis distance measure between the i^{th} pixel and the centroid of class l, and which is described by $R_{il} = \|X_i - \bar{X}_l\|_{\Sigma_l^{-1}} = (X_i - \bar{X}_l)^T \xi_l^{-1} (X_i - \bar{X}_l)$ where $X_i = (R_i, G_i, B_i)$ is the 3-dimensional feature vector of the i_{th} pixel composed with the Red, Green and Blue components. $\bar{X}_l$ is the 3-dimensional centroid vector of class l, and Σ_l is the covariance matrix of class l. By combining the motion equation with the energy function, we get a set of neural dynamics described by $\frac{\partial U_{il}}{\partial t} = -\alpha(t) R_{il}^2 V_{il}$

The input-output function for the cell that assigns a label m to the i^{th} pixel is given by:

$$\begin{array}{l} V_{im}(t+1) = 1, \quad if\ U_{im} = Max[U_{il}(t), \forall l] \\ V_{il}(t+1) = 0, \quad for\ l \neq m \end{array} \tag{1}$$

The algorithm proceeds as follows:1)Initialize the input

of neurons to random values. 2) Apply the input-output relation to obtain the new output values for each neuron, establishing thus the assignment of pixels to classes. 3) Compute the centroid $\bar{X}_l$ and the covariance matrix Σ_l for each class l as follows: $\bar{X}_l = \frac{\Sigma_{i=1}^{N} X_i V_{il}}{\Sigma_{i=1}^{N} V_{il}}$
$\xi_l = \frac{\Sigma_{i=1}^{N} V_{il}(X_i - \bar{X}_l)(X_i - \bar{X}_l)^T}{\Sigma_{i=1}^{N} V_{il}}$
4) Update the input of each neuron according using the Euler's approximation: $U_{il}(t+1) = U_{il}(t) - \alpha(t) R_{il}^2 V_{il}$. Here, neuron input weights are adjusted in an attempt to reduce the output error to end up with an optimal or near optimal segmentation map. 5) repeat from step 2 until convergence. The convergence condition is set to the number of iterations exceeds a certain number.

The classified image might exhibit a "salt-and-paper" appearance due to the spectral variability of PCO image. This phenomena might inflate the number of regions considerably. To reduce this effects, we apply a median filter on the clustered image. The size od the filter controls the amount of smoothness.

4 Experiments

The classification was applied on a variety of 20 PCO images (Figure 2, 1st column depicts some samples, the first image corresponds to a safe case). The aim of the experiments was to check how the number of regions varies with respect to the number of clusters and the size of the median filter, and eventually to what extent such number can reflect the amount of PCO.

A series of trials were conducted, whereby the number of classes was set respectively to 3,4,5,6. Each series was conduced with a median filter of a different size, namely, 3x3 5x5 7x7 and 9x9 size. Figure 2(a) (columns 2 to 5) depicts samples of images clustering obtained with a median filter of 3x3 size. Each cluster is displayed with a different color). The preservation of integrity of the background by the clustering process is a noticeable aspect of the method and shows evidence of the near optimal solution that the algorithm can reach. It is interesting to note that the reflections areas, in the last image have been detected as a single compact region, and in some sense have been "isolated". This suggest that our assessment technique, is expected not to be seriously affected by such regions as it does rather consider their numbers rather than their sizes. For each clustered image we extracted the number of regions. Figure 2(b) depicts the distribution of the number of regions, for a 3×3 median filter, across the 20 images. We notice that the variations of the number of regions across the images exhibit sensibly the same profile across all the numbers of clusters. In another experience, we calculated for each image, 50 estimations of the number of regions, and calculated the relative standard deviation (σ/μ) where μ and σ are respectively the mean and the standard deviation of the 50 estimations. The results are depicted in Figure 2(c). We can see that the maximum relative standard deviation does not exceed 10 %. This aspect is very interesting as it permits to fulfill the repeatability requirement needed in a PCO grading system.

These remarkable stability properties of the number of regions, encourage us to propose it as a tool for differentiating and distinguishing between the PCO level in different images. We tested this measurement tool by comparing the corresponding assessment with a medical expertise evaluation, that involved three observes. For this purpose, we brought the number of regions, extracted from all the images at each trial (with 3,4,5 and six clusters), down to the standard medical range [0-4]. This is a discrete range when the possible PCO level score can be either 0 (no PCO), 1 (mild), 2 (average) 3(strong) and 4 (severe). Few samples of the results (because of the limited space) are depicted in Figure 2(d), where the medical expertise assessment is plotted together with each of the gradings obtained from the four trials. We notice that the variation profile of the medical expert grading and our approach's grading exhibit clear similarities across all the series of trials, despite some disparities at some instances. We believe that this emanated form the border cases where it is hard for a human assessor to make sharp distinction.

Still In Figure 2(d), we notice that our approach produces a valid score, across all the trials for the image labelled by number 19. It is the image showing reflection areas(figure 2(a) last row). This confirms the robust aspect of our approach with respect to light artifacts and reflections, eventually within a reasonable limits.

Figure 2(e) depicts the correlation coefficient between the medical expert grading and our approaches's grading, for each size of the deployed median filter and across the different numbers of clusters. We observe that the overall best correlation is obtained by the 3x3 and 5x5 size median filters. For the 3 cluster, all the correlations look reasonable. The 9x9 median filter produces the least correlation. This can be explained as a result of a combination of an over-smoothing due to the large size of the filer and the over-segmentation inferred by the large number of clusters.

5 Conclusion

In this work, we proposed a new approach for assessing PCO level from Digital images. Contrary to previous approaches that attempted to address the hard problem of extracting and measuring the textured areas, our approach avoids the segmentation issues, and propose an analysis techniques based on simple concepts. It is fully automatic and does not require any manual intervention. The hypothesis that a simple statistical feature, namely the number of regions, in the output image of the standard *k-means* clustering technique is a potential grading tool for assessing amount of PCO in digital images, has been confirmed by the comparison with medical expertise assessment. The Hopfield-like neural network system is implemented with a non optimized Matlab and C++ (Mex files). Convergence is ensured in an average of 120 iterations, lasting about 30 seconds, on a Pentium 4, 3.2 GHz. This makes the approach suitable for interactive application. We believe that the classified images still carry

other features that are worth to examine, for instance the distribution of the regions in the image, as ophthalmologists suspect some relationship between the PCO distribution (particularity with respect to the center of the capsule) and the visual acuity. The analysis of the geometrical and topological properties of the regions in the segmented images might be also useful in determining the type of PCO. We are currently investigating these aspects.

Acknowledgements

We would like to thank Dr Tariq Aslam from the Manchester Eye Hospital, UK for providing the PCO images and Dr. Prashant Bhatia and his colleagues in the Ophthalmology Department at Welcare Hospital, for their kind collaboration and feedback.

References

[1] D.J Spalton, "Posterior capsular opacification after cataract surgery", Eye, 13 (Pt 3b), June, 1999, pp.489-492.

[2] M.S. Lasa, et al "Scheimpflug photography and postcataract surgery posterior capsule opacification" Journal of Ophthalmic Surgery. No. 26, pp.110-113, 1995.

[3] K. Hayashi et al , "In vivo quantitative measurement of posterior capsule opacification after extracapsular cataract surgery", American Journal of Ophthalmology, Vol. 125, No.6, pp. 837-843, 1998.

[4] M.R. Tetz et al , "Photographic Image Analysis System, of Posterior Capsule Opacification". Journal of Cataract Refract Surgery, Vol. 23, pp.1515-1520, 1997.

[5] P.G. Ursell et al, "Relationship between intraocular lens biomaterials and posterior capsule opacification", Journal of Cataract Refract. Surgery, Vol. 24, pp.352-360. 1998.

[6] M.C. Wang, et al "Digital Retroilluminated Photography to analyze posterior capsule opacification in eyes with intraocular lenses". Journal of Cataract Refract. Surgery, Vol. 26, pp,56-51, 2000

[7] D.S. Friedman et al, "Digital Image Capture and Automated Analysis of Posterior Capsular Opacification". Investigative Ophtalmolology Vision Sciences Vol. 40, pp.1715-1726, 1999.

[8] B. Barman et al, "Quantification of Posterior, Capsular Opacification in digital Images after Cataract Surgery". Investigative Ophthalmology Vision Sciences, Vol. 41, pp.3883-3892, 2000.

[9] A.P. Paplinski et al, "Segmentation of a class of ophthalmological images using a directional variance operator and co-occurrence arrays", Optical Engineering, Vol. 36, pp.3140-3147, November 1997.

[10] H. Siegl et al, "Assessment of posterior capsule opacification after cataract surgery", Proceedings 12th SCIA, Scandinavian Conference on Image Analysis, Bergen, pp. 54-61 (2001)

[11] O. Findl et al , "Comparison of 4 methods for quantifying posterior capsule opacification" J Cataract Refract Surgery, Vol. 29, pp.106-111, 2003.

[12] T. Aslam, "A freely accessible, evidence based, objective system of analysis of posterior capsular opacification; evidence for its validity and reliability" BMC Ophthalmology, Vol. 5, No.1, pp.1-10., 2005.

[13] D. MacKay, Information Theory, Inference and Learning Algorithms, Cambridge University Press, 2003.

[14] B. Kagamar-Parsi et al , "Clustering with neural networks", Biological Cybernetics, vol. 61, pp. 201-208, 1990.

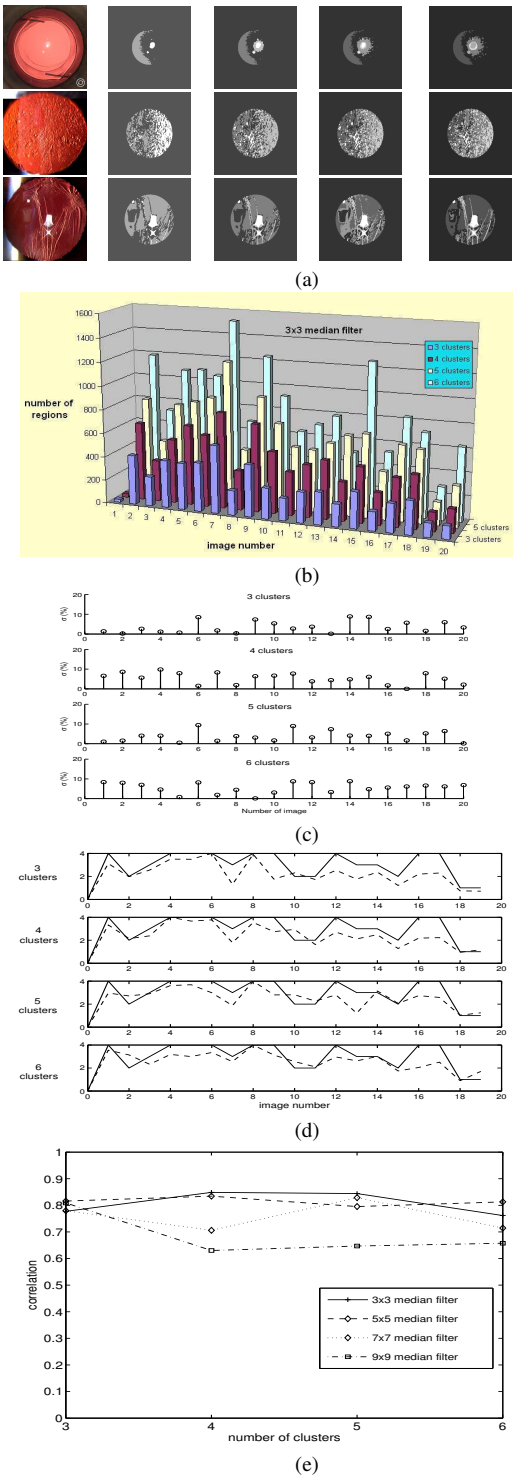

Figure 2: a:samples of PCO images (1s column), and classification results obtained for a number of classes equal to 3, 4, 5 and 6. b:Number of regions in the clustered image. c:Standard deviation (σ) of 50 estimation of number of regions. d:Comparison between a medical expert grading (solid line) and our approach grading (dashed line) for a number of clusters equal to 3,4,5 and 6. e: Correlation factor between the medical expert grading and our approach's grading.